

to define such correlations between chlorin structure and their vibrational properties.

The findings reported here support our hypothesis and previous observations that vibrational spectroscopy, and especially resonance Raman spectroscopy, can be diagnostic for the chlorin macrocycle.^{19,21} The spectral criteria that distinguish chlorins from porphyrins appear to hold not only for a large variety of ring substitution patterns and different central metal ions but also when metallochlorins occur as prosthetic groups in metalloproteins. Extension of this work to the analysis of the vibrational properties of bacteriochlorins and isobacteriochlorins (tetrahydroporphyrins)

is in progress. These techniques should make it possible to characterize systems that are not amenable to prosthetic group extraction.

Acknowledgment. This research was supported by the National Institutes of Health (GM 34468 to T.M.L. and C.K.C.). We thank Prof. K. M. Kadish for his generous gifts of the NiTMP and NiTMC complexes. We also thank Linda Schmidlin for technical assistance.

Registry No. Cu^{II}TPP, 14172-91-9; Cu^{II}TPC, 52064-15-0; Ni^{II}TMC, 75758-44-0; Ni^{II}TMP, 67067-51-0.

Redox Properties of Metalloporphyrin Dimers

James P. Collman,* Jacques W. Prodnollet,[†] and Charles R. Leidner

Contribution from the Department of Chemistry, Stanford University, Stanford, California 94305. Received October 7, 1985

Abstract: Cyclic and rotated disk voltammetry of two metalloporphyrin dimers, [Ru(OEP)]₂ and [Os(OEP)]₂, exhibit four oxidations and two reductions for each compound which are all chemically and electrochemically reversible on the voltammetric time scale. Comparison of the formal potentials of the six couples suggests that the first two oxidations are metal-centered redox processes; the remaining four couples are likely to be ligand centered. Controlled chemical oxidations using ferricinium hexafluorophosphate, silver tetrafluoroborate, and tris(4-bromophenyl)ammonium hexachloroantimonate cleanly generate the monocations [M(OEP)]₂⁺ and the dications [M(OEP)]₂²⁺. NMR, ESR, and electronic spectroscopy of these dimeric, cationic products support the assignment of the two oxidations as metal centered. These oxidations permit the preparation of the two series of metalloporphyrin dimers: paramagnetic [M(OEP)]₂ with bond order = 2, paramagnetic [M(OEP)]₂⁺ with bond order = 2.5, and diamagnetic [M(OEP)]₂²⁺ with bond order = 3.

We have recently developed a new class of binuclear metal complexes M₂L₈ where two metalloporphyrins are joined by a multiple metal–metal bond.^{1–3} These dimers were analyzed in terms of a simple molecular orbital diagram (Figure 1), proposed by Cotton^{4,5} for quadruply bonded systems. This scheme accounts for the ground-state geometry, spin state, and bond order of these dimers solely on the basis of the total number of valence d electrons. The rigid nature of the porphyrin macrocycle, which requires a planar or nearly planar geometry about each metal center, allows the variation of the metal–metal bond orders in these complexes without the interference of bridging ligands, permitting a systematic study of the resulting structural, spectroscopic, and chemical characteristics over the entire bond order range.

Variation of the metal–metal bond orders can be achieved by three different methods: (i) Coupling of two metalloporphyrin monomers containing the same metal in the same oxidation state, M(II), affords the neutral homodimers. Singly (M = Rh,^{6,7} Ir⁸), doubly (M = Ru,¹ Os²), and quadruply (M = Mo,² W³) bonded homodimers have been prepared by this technique, but the triply bonded Tc and Re analogues are still unknown. So far only the ruthenium homodimer [Ru(OEP)]₂ has been structurally characterized.⁹ Furthermore, we were able to measure the rotational barrier of the Mo–Mo quadruple bond in meso-substituted molybdenum(II) dimers.¹⁰ (ii) Coupling of two metalloporphyrin monomers containing different metals in the same oxidation state should yield neutral heterodimers. This method was used to prepare the only known example of a porphyrin heterodimer containing two transition metals,¹¹ (OEP)Ru=Os(OEP). This compound, which was observed by ¹H NMR, has not been isolated.² (iii) Oxidation or reduction of either homo- or heterodimers is a potentially attractive way of preparing ionic dimers with altered metal–metal bond order. This procedure, which has never

been used for metalloporphyrin dimers, is the subject of the present paper.

Herein we report the electrochemical and chemical investigation of the redox properties of [Ru(OEP)]₂ and [Os(OEP)]₂.

Results and Discussion

Electrochemistry of [Ru(OEP)]₂ and [Os(OEP)]₂. Considerable effort has been made during the last 20 years to understand the redox behavior of metalloporphyrin monomers.¹² It is now recognized that oxidation (or reduction) can occur either at the porphyrin macrocycle, to generate an organic π cation (or π anion) radical, or at the metal center itself to induce oxidation state changes.¹² However, fewer electrochemical studies on metal–metal bonded complexes have been reported.^{13–16} This

(1) Collman, J. P.; Barnes, C. E.; Collins, T. J.; Brothers, P. J. *J. Am. Chem. Soc.* **1981**, *103*, 7030.

(2) Collman, J. P.; Barnes, C. E.; Woo, L. K. *Proc. Natl. Acad. Sci. U.S.A.* **1983**, *80*, 7684.

(3) Collman, J. P.; Woo, L. K., unpublished results.

(4) Cotton, F. A.; Curtis, N. F.; Harris, C. B.; Johnson, B. F. G.; Lippard, S. J.; Mague, J. T.; Robinson, W. R.; Wood, J. S. *Science (Washington, D.C.)* **1964**, *145*, 1305.

(5) Cotton, F. A. *Inorg. Chem.* **1965**, *4*, 334.

(6) Ogoshi, H.; Setsune, J.; Yoshida, Z. *J. Am. Chem. Soc.* **1977**, *99*, 3869.

(7) Wayland, B. B.; Newman, A. R. *Inorg. Chem.* **1981**, *20*, 3093.

(8) Collman, J. P.; Leidner, C. R.; Garner, J. M.; Johnson, K., unpublished results.

(9) Collman, J. P.; Barnes, C. E.; Sweptson, P. N.; Ibers, J. A. *J. Am. Chem. Soc.* **1984**, *106*, 3500.

(10) Collman, J. P.; Woo, L. K. *Proc. Natl. Acad. Sci. U.S.A.* **1984**, *81*, 2592.

(11) The preparation of a heterometallic porphyrin dimer containing a transition metal and a main group element, (OEP)Rh–In(OEP), has recently been reported by Jones and Wayland (Jones, N. L.; Wayland, B. B. *Abstracts of Papers*, 189th ACS National Meeting of the American Chemical Society; Miami Beach, FL; American Chemical Society: Washington, DC 1985; Abstract 56).

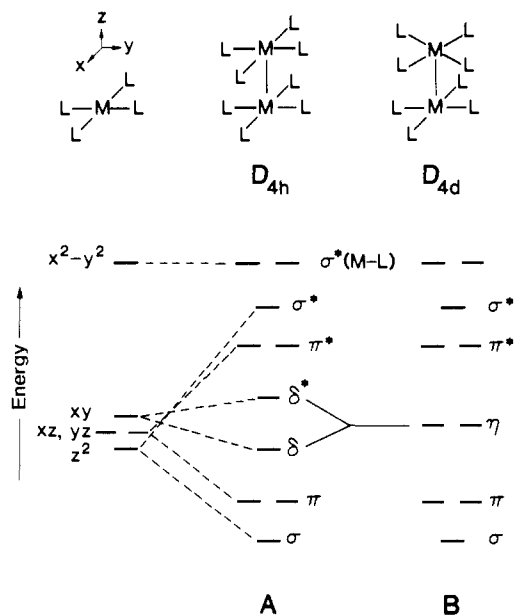
(12) Davis, D. G. In *The Porphyrins*; Dolphin, D., Ed.; Academic Press: New York, 1978; Vol. V, p 127.

[†] Present address: Institut de Chimie Minérale et Analytique, 3 place du Chateau, CH-1005 Lausanne, Switzerland.

Table I. Half-Wave Potentials of [Ru(OEP)]₂ and [Os(OEP)]₂^a

	$E_{1/2}$	[Ru(OEP)] ₂		[Os(OEP)] ₂	
		DME ^b	CH ₂ Cl ₂ ^c	DME ^b	CH ₂ Cl ₂ ^c
[M ^{III,III} (OEP)] ₂ ³⁺ - e ⇌ [M ^{III,III} (OEP)] ₂ ⁴⁺	$E_{1/2}(1)$	1.30 ^d	1.22	1.19	1.16
[M ^{III,III} (OEP)] ₂ ²⁺ - e ⇌ [M ^{III,III} (OEP)] ₂ ³⁺	$E_{1/2}(2)$	1.15 ^d	1.03	1.08	0.99
[M ^{III,III} (OEP)] ₂ ⁺ - e ⇌ [M ^{III,III} (OEP)] ₂ ²⁺	$E_{1/2}(3)$	0.62	0.50	0.09	-0.01
[M ^{II,III} (OEP)] ₂ - e ⇌ [M ^{III,III} (OEP)] ₂ ⁺	$E_{1/2}(4)$	-0.11	-0.46	-0.53	-0.77
[M ^{II,II} (OEP)] ₂ + e ⇌ [M ^{II,II} (OEP)] ₂ ⁻	$E_{1/2}(5)$	-1.02	-1.32	-1.18	-1.43
[M ^{II,II} (OEP)] ₂ ⁻ + e ⇌ [M ^{II,II} (OEP)] ₂ ²⁻	$E_{1/2}(6)$	-1.51 ^d	e	-1.66	e

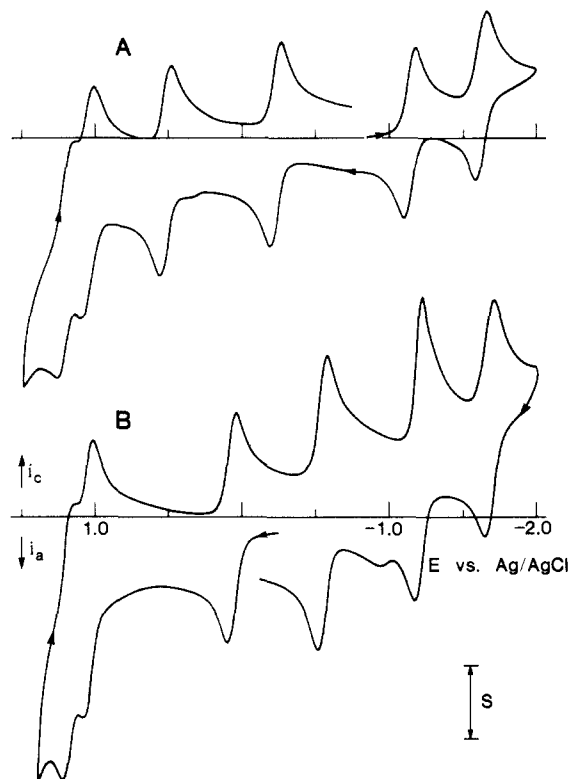
^a $E_{1/2}$ in V vs. Ag/AgCl. ^b Done in 0.8 M Bu₄NClO₄/DME. ^c Done in 0.2 M Bu₄NClO₄/CH₂Cl₂. ^d Some degradation after 3 min. ^e Voltammetric wave in solvent discharge.

Figure 1. Qualitative molecular orbital diagram for the metal-metal bonding in M₂L₈ complexes.

is an elegant method of varying the metal-metal bond order.^{13,15} Consequently, one could expect a rich electrochemistry for these 4d and 5d metalloporphyrin dimers, since both ligand- and metal-centered redox processes are possible.

The electrochemistry of [Ru(OEP)]₂ and [Os(OEP)]₂ was studied in dimethoxyethane (DME) and dichloromethane. The cyclic voltammogram response of the two dimers in 0.8 M Bu₄NClO₄/DME is shown in Figure 2. Six chemically and electrochemically reversible one-electron redox couples are evident for each compound; the half-wave potentials ($E_{1/2}$) for each couple are displayed in Table I. Rotated disk voltammetry indicates that the six couples are comprised of four oxidations and two reductions for each compound. Exhaustive electrolyses at constant potential were not feasible because of solubility and decomposition problems. Therefore, we could not characterize spectroscopically the new species generated in situ. Despite this difficulty, the data in Figure 2 permit the tentative assignment of $E_{1/2}(3)$ and $E_{1/2}(4)$ as metal-centered oxidation, whereas $E_{1/2}(1)$, $E_{1/2}(2)$ and $E_{1/2}(5)$, $E_{1/2}(6)$ are ligand oxidation and reduction, respectively.

Fuhrhop's study^{17,18} of the redox properties for 30 different metalloporphyrin monomers revealed that the difference in $E_{1/2}$'s between the first ring oxidation and the first ring reduction is invariably equal to 2.25 ± 0.15 V.¹⁷ Values of 2.17 V for [Ru-

Figure 2. Cyclic voltammogram response of [M(OEP)]₂ in 0.8 M Bu₄NClO₄/DME at 100 mV/s: (A) 0.8 mM [Ru(OEP)]₂, $S = 18 \mu\text{A}/\text{cm}^2$; (B) 0.2 mM [Os(OEP)]₂, $S = 68 \mu\text{A}/\text{cm}^2$.

(OEP)]₂ and 2.26 V for [Os(OEP)]₂ are obtained for the parameter $E_{1/2}(2) - E_{1/2}(5)$, suggesting that $E_{1/2}(2)$ represents the first oxidation potential of one of the porphyrin rings in the dimers and $E_{1/2}(5)$ the first reduction potential. Fuhrhop has also found that divalent metals afford a linear relationship between either the first oxidation or reduction potential at the ring and the electronegativity of the central metal ion.¹⁸ Since the electronegativities of ruthenium and osmium are identical (2.2),¹⁹ the half-wave potentials for the ring redox reactions should be the same within ~0.1 V for the ruthenium and osmium dimers. This is in fact observed; $E_{1/2}(1, 2, 5, 6)$ exhibit only a small variation (<0.16 V), conversely $E_{1/2}(3)$ and $E_{1/2}(4)$ are strongly dependent on the nature of the metal ion and can confidently be assigned to the metal oxidation potential (M(II/III)).

Our assignments are also consistent with the results obtained for the six-coordinate monomers, Ru(OEP)L₂ (L = py, PⁿBu₃). Both compounds undergo two reversible oxidations in dichloromethane at $E_{1/2}(M) = 0.08$ V and $E_{1/2}(R) = 1.05$ V (vs. SSCE) for Ru(OEP)py₂²⁰ and at $E_{1/2}(M) = 0.03$ V and $E_{1/2}(R) = 1.20$ V (vs. Ag/AgCl) for Ru(OEP)(PⁿBu₃)₂.²¹ In each case

(13) Cotton, F. A.; Walton, R. A. In *Multiple Bonds Between Metal Atoms*; Wiley: New York, 1982.

(14) Dessy, R. E.; Weissman, P. M.; Pohl, R. L. *J. Am. Chem. Soc.* **1966**, *88*, 5117.

(15) Chavan, M. Y.; Feldman, F. N.; Lin, X. Q.; Bear, J. L.; Kadish, K. M. *Inorg. Chem.* **1984**, *23*, 2373.

(16) Chavan, M. Y.; Zhu, T. P.; Lin, X. Q.; Ahsan, M. Q.; Bear, J. L.; Kadish, K. M. *Inorg. Chem.* **1984**, *23*, 4538.

(17) Kadish, K. M.; Davis, D. G.; Fuhrhop, J.-H. *Angew. Chem.* **1972**, *84*, 1072.

(18) Fuhrhop, J.-H.; Kadish, K. M.; Davis, D. G. *J. Am. Chem. Soc.* **1973**, *95*, 5140.

(19) Pauling, L. In *The Nature of the Chemical Bond*, 3rd ed. Cornell University: New York, 1960; p 93.

(20) Brown, G. M.; Hopf, F. R.; Ferguson, J. A.; Meyer, T. J.; Whitten, D. G. *J. Am. Chem. Soc.* **1973**, *95*, 5939.

(21) Barley, M.; Becker, J. Y.; Domazetis, G.; Dolphin, D.; James, B. R. *Can. J. Chem.* **1983**, *61*, 2389.

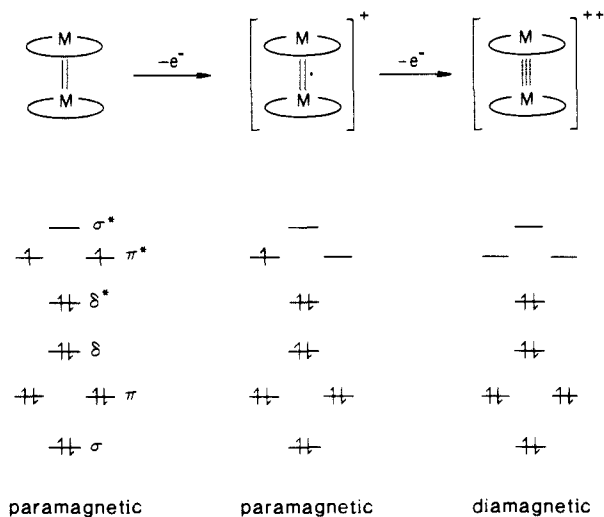


Figure 3. Oxidation induced variations of the bond order and magnetic properties in d^6 metal(II) porphyrin dimers.

the wave at the lower potential ($E_{1/2}(M)$) is attributed to a metal-centered oxidation, whereas ring oxidation occurs at higher voltage ($E_{1/2}(R)$). The values of $E_{1/2}(1)$ and $E_{1/2}(3)$ obtained for the ruthenium dimer are similar to $E_{1/2}(M)$ and $E_{1/2}(R)$, and we think they are related to the same phenomenon. Furthermore, it was found that a metal oxidation occurred at $E_{1/2}(M) = -0.40$ V for Os(OEP)py₂,²⁰ this value is very close to $E_{1/2}(1)$ obtained for [Os(OEP)]₂. These indirect comparisons support the above arguments.

It is interesting to note that when the metal oxidations occur the dimeric nature of the starting material is retained, but the bond order of the metal-metal bond should be modified. Based on Cotton's MO diagram, the first oxidation should generate an 11 d-electron mixed-valence monocation, the ground state electronic configuration of which is $\sigma^2\pi^4\delta^2\delta^*2\pi^*$, and should result in a paramagnetic species with a metal-metal bond order of 2.5 (Figure 3). The product of the second oxidation should be a diamagnetic 10 d-electron dication with an electronic configuration of $\sigma^2\pi^4\delta^2\delta^*2$ representing a formal triple bond between the two metal ions (Figure 3). Compounds with a Ru₂⁵⁺ core are well-known in the case of non-porphyrin ligands,¹³ but their osmium analogues as well as species containing triply bonded Ru or Os atoms are rare.^{13,15,22-24} By using these initial assignments as a starting point we then studied the chemical reactivity of the neutral dimers toward three different homogeneous oxidants: AgBF₄, ferrocenium hexafluorophosphate ([FeCp₂](PF₆)), and tris(4-bromophenyl)ammonium hexachloroantimonate (TBPAAH). The results of this study are presented in the next section.

Chemical Oxidation of [Ru(OEP)]₂ and [Os(OEP)]₂. Syntheses. The formal potentials of AgBF₄, [FeCp₂](PF₆), and TBPAAH²⁵ suggest that, if unusual solvent effects do not occur, these reagents should oxidize the neutral dimer selectively by a two-electron process without affecting the π electrons of the porphyrin macrocycle (ring oxidation). In principle, by controlling the stoichiometry, the reaction can be limited to a single oxidation and thereby generate the mixed-valence monocations.

Single-electron oxidations were performed at room temperature by treating a benzene solution of each dimer with 1 equiv of

Scheme I

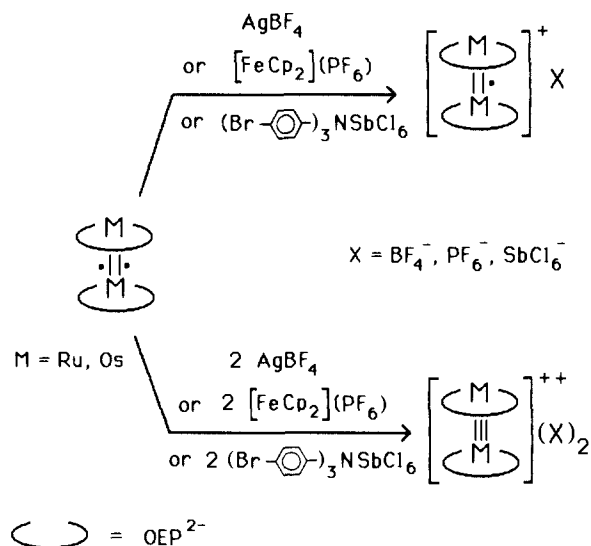


Table II. Comparison between the Observed Isotropic NMR Chemical Shifts²⁶ for Neutral ([M(OEP)]₂) and Monocationic ([M(OEP)]₂⁺) Dimers

	H _{meso}	CH ₂		CH ₃
[Ru(OEP)] ₂ ^{a,b}	0.90	21.30	7.00	1.50
[Ru(OEP)] ₂ ^{+c}	3.71	5.42	1.65	0.40
[Os(OEP)] ₂ ^a	-10.28	7.06	3.83	0.22
[Os(OEP)] ₂ ^{+c}	0.71	1.95	1.15	-0.02

^aToluene-*d*₈, 25 °C. ^bFrom ref 9. ^cCD₂Cl₂, 25 °C.

oxidizing agent (Scheme I). The resulting cations were each isolated in good yield as purple solids precipitating out of solution. When 2 two equiv of oxidant are used, a second oxidation occurs (Scheme I), and dicationic dimers of formula [M(OEP)]₂(X)₂ have been isolated in almost quantitative yields as purple (Ru) or brown (Os) solids. Satisfactory elemental analyses were obtained for all new compounds (except for 11), but attempts to determine their molecular weight by mass spectrometry have not been successful, due to degradation.

Electrochemistry. The cyclic voltammetry of all oxidized products in 0.2 M Bu₄NClO₄/CH₂Cl₂ is identical with that of the neutral dimers obtained under the conditions. The dimeric nature of the starting material is, therefore, retained after one- or two-electron oxidation. The rotated disk voltammetry of the compounds verified that one- and two-electron oxidations for the mono- and dicationic dimers, respectively, had occurred. The electrochemical results are fully consistent with the proposed mono- or dicationic dimeric formulas.

¹H NMR. The ¹H NMR spectra of the monooxidized products (1-3 and 7-9) are all indicative of paramagnetic dimeric OEP complexes. This is expected from the qualitative MO diagram presented in Figure 3. For the same metal the chemical shifts are almost insensitive to the nature of the counterion. The overall appearance of the spectra indicates that (i) these complexes possess a fourfold symmetry; (ii) the porphyrin ring was not degraded by oxidation; and (iii) the α -methylene proton resonances of the OEP ligand appear as two different signals, consistent with a dimeric structure which lacks mirror symmetry at the porphyrin plane. Furthermore, the observed isotropic shifts²⁶ for all cationic complexes are much smaller than for the neutral precursors (Table II). Their temperature dependence was also found to be linear over a temperature range -90 to +30 °C. The adherence of all shifts to the Curie Law indicates that these dimers exist in a single spin state over the entire temperature range studied. This was

(22) Warren, L. F.; Goedken, V. L. *J. Chem. Soc., Chem. Commun.* **1978**, 909.

(23) Tetrick, S. M.; Coombe, V. T.; Heath, G. A.; Stephenson, T. A.; Walton, R. A. *Inorg. Chem.* **1984**, *23*, 4567.

(24) Chakravarty, A. R.; Cotton, F. A.; Tocher, D. A. *Inorg. Chem.* **1985**, *24*, 1334 and references therein.

(25) $E_{1/2}$ (vs. Ag/AgCl) from cyclic voltammetry in approximately 10⁻³ M solution of the oxidant in 0.2 M Bu₄NClO₄/CH₂Cl₂: AgBF₄ (ca. 0.67 V), [FeCp₂](PF₆) (0.37 V), and TBPAAH (ca. 1.06 V). Note that [Cp₂Fe](PF₆) is incapable thermodynamically of oxidizing [Ru(OEP)]₂⁺ (Table I), however, the lower solubility of [Ru(OEP)]₂(PF₆)₂ compared to [Ru(OEP)]₂(PF₆) drives the equilibrium toward complete oxidation.

(26) The observed isotropic shifts were obtained by the method reported in ref 9: $\delta_{\text{iso}}^{\text{obsd}} = \delta_{\text{iso}}^{\text{para}} - \delta_{\text{iso}}^{\text{dia}}$, where $\delta_{\text{iso}}^{\text{para}}$ is the observed shift of a given proton and $\delta_{\text{iso}}^{\text{dia}}$ is the corresponding shift of the diamagnetic reference compound² [Rh(OEP)]₂.

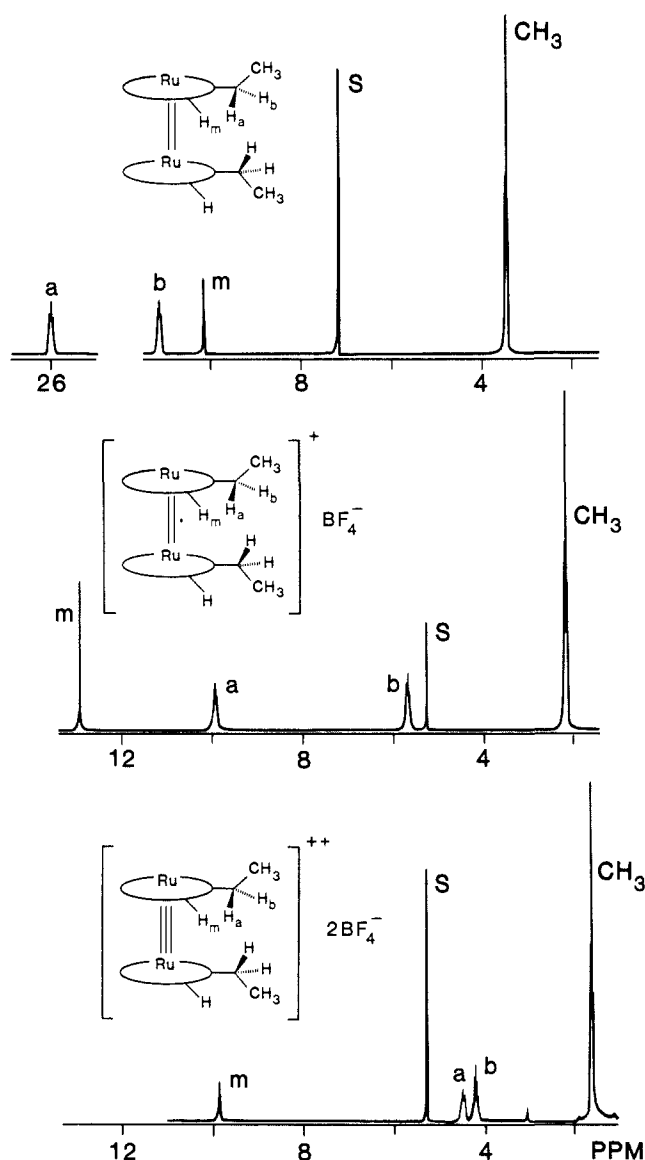


Figure 4. ^1H NMR spectra (300 MHz, $T = 25^\circ\text{C}$) of Ru porphyrin dimers: (A) $[\text{Ru}(\text{OEP})]_2$ in benzene- d_6 ; (B) $[\text{Ru}(\text{OEP})]_2(\text{BF}_4)$ in CD_2Cl_2 ; (C) $[\text{Ru}(\text{OEP})]_2(\text{BF}_4)_2$ in CD_2Cl_2 . S = residual solvent protons.

previously found for $[\text{Ru}(\text{OEP})]_2$,⁹ which has been shown to be a ground-state triplet.

The ^1H NMR spectra of the dioxidized products (4–6 and 10–12) are all indicative of diamagnetic OEP complexes. Again, this is predicted by the MO diagram (Figure 3). The chemical shifts are almost insensitive to the nature of the metal and the counterion, and like the monocations, the overall appearance of the spectra is consistent with fourfold symmetrical dimeric compounds. We have also verified that the chemical shifts are temperature independent. This is consistent with our proposal that these dicationic dimers are diamagnetic. For comparison, the ^1H NMR spectra of $[\text{Ru}(\text{OEP})]_2$, $[\text{Ru}(\text{OEP})]_2\text{BF}_4$, and $[\text{Ru}(\text{OEP})]_2(\text{BF}_4)_2$ are given in Figure 4.

Electronic Spectra. UV-vis spectra have been recognized as one of the most powerful tools to distinguish between ring vs. metal oxidation in metalloporphyrin monomers. A spectrum with a single broad band covering the whole visible range and a Soret peak of much lower intensity compared with the unoxidized precursor seem to be characteristic of an organic π radical.^{18,27,28} However, if the typical spectrum of the starting material is retained after oxidation, it can be assumed that oxidation has occurred at the metal.^{18,21,27,28}

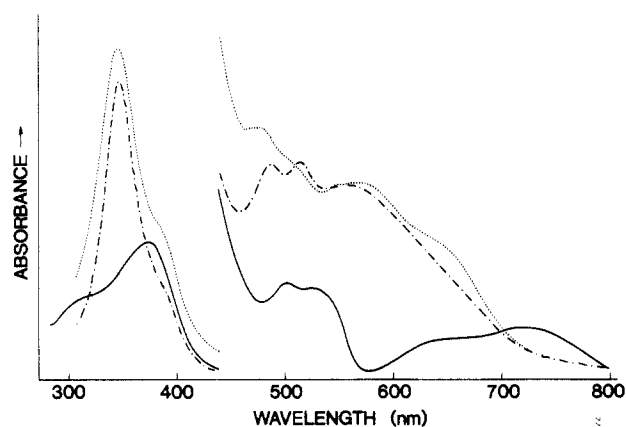


Figure 5. Electronic spectra at 25°C of $[\text{Ru}(\text{OEP})]_2$ in benzene (—), $[\text{Ru}(\text{OEP})]_2(\text{BF}_4)$ in CH_2Cl_2 (···), and $[\text{Ru}(\text{OEP})]_2(\text{BF}_4)_2$ in CH_2Cl_2 (-·-·).

The visible spectra of the neutral dimers consist only of large, poorly resolved bands. Thus, if the same criteria as the monomers can be applied in this case, we do not expect to see many changes either for ring or for metal oxidation. On the other hand, the differences in the intensity of the Soret peaks should allow us to assess this point. Optical spectra of all monooxidized products show modest variations in the visible region compared with the neutral dimers, but the fact that the Soret peak is even more intense (except for 6) might indicate that oxidation occurred at the metal. Furthermore, the spectra of all dioxidized products are very similar (visible and Soret) to those obtained for monocations. This confirms that the second oxidation is also metal centered. As an example the optical spectra of $[\text{Ru}(\text{OEP})]_2$, $[\text{Ru}(\text{OEP})]_2\text{BF}_4$, and $[\text{Ru}(\text{OEP})]_2(\text{BF}_4)_2$ are displayed in Figure 5.

ESR. ESR is also a powerful tool for assigning the site of oxidation in metalloporphyrin monomers. Very sharp signals with a line width of less than 10 G are indicative of organic π cation radicals, while much broader signals with large hyperfine splitting are characteristic of metal-centered radicals.^{18,29}

ESR spectra of the mono- and dioxidized species in dichloromethane glasses at 77 K show no detectable signal. We believe that in both cases this lack of an ESR signal attributable to a π cation radical favors the metal oxidation mechanism. This argument has been used by several workers to assess the site of the first oxidation of Ru(II) porphyrin^{20,21} and phthalocyanine³⁰ complexes. It should be noted that problems in the detection of ESR signals of Ru(III) species were also reported by these authors.^{20,30}

Summary and Conclusions

The electrochemical experiments presented herein illustrate the rich redox chemistry of $[\text{Ru}(\text{OEP})]_2$ and $[\text{Os}(\text{OEP})]_2$. Cyclic voltammetry and rotated disk voltammetry indicate that both dimers exhibit four facile oxidations and two facile reductions. Particularly interesting are the first two oxidations, which are attributed to metal-centered redox reactions; the other couples are probably ligand centered. In order to verify the assignments of the first two oxidation waves, controlled chemical oxidations of these dimers were performed, and the nature of the resulting isolated products was analyzed by electrochemical (CV, RDE) and spectroscopic (^1H NMR, UV-vis, ESR) methods. All of these results are consistent with our assertion that the first oxidation generates cationic paramagnetic mixed-valence metalloporphyrin dimers of the formula $[\text{M}^{\text{II,III}}(\text{OEP})]_2^+$. According to the MO diagram developed to understand the metal-metal bonding in the neutral dimers, these complexes should possess a Ru-Ru (or Os-Os) multiple bond with a bond order of 2.5. The second

(27) Fuhrhop, J.-H. *Struct. Bonding (Berlin)* **1974**, *18*, 1.

(28) Fuhrhop, J.-H. In *Porphyrins and Metalloporphyrins*; Smith, K. M., Ed.; Elsevier Scientific: New York, 1976; p 609.

(29) Felton, R. H. In *The Porphyrins*; Dolphin, D., Ed.; Academic Press: New York, 1978; Vol. V, p 53.

(30) Dolphin, D.; James, B. R.; Murray, A. J.; Thornback, J. R. *Can. J. Chem.* **1980**, *58*, 1125.

oxidation yields diamagnetic dicationic metalloporphyrin dimers of the formula $[M^{III,III}(OEP)]_2^{2+}$ representing a formal M–M triple bond. Such electrochemical tuning of the metal–metal bond order has been recently reported for an unrelated (non-porphyrinic) dinuclear ruthenium acetamide complex.²² To our knowledge, there is only one other report of complexes containing Os–Os bonds with bond orders of 2.5²³ and two compounds with Ru–Ru triple bonds.^{15,22} The latter complexes have not been fully characterized. Attempts are underway to grow crystals of the new multiply bonded dimers suited for X-ray diffraction studies in order to determine their exact geometries and, particularly, their metal–metal bond lengths.

Not only has this study produced novel metalloporphyrin dimers and examined the redox chemistry of some metal–metal bonded compounds, but it also has opened up new areas of study. One such development in this project is the opportunity to study the homogeneous electron transfer properties of metal–metal bonded compounds. Our preliminary results indicate that the NMR spectra of solutions containing certain redox pairs, such as $[Os(OEP)]_2^+$ and $[Os(OEP)]_2^{2+}$, exhibit line broadening and changes in chemical shifts which are indicative of rapid electron transfer self exchange. We are currently pursuing this interesting line of research. Additionally, the oxidized dimers provide synthetic routes to novel metalloporphyrin monomers. In the same way that the neutral dimers can be considered to be “naked” Ru(II) and Os(II) porphyrin monomers,³¹ the new triply bonded dications can be viewed as precursors to Ru(III) and Os(III) monomers. Investigation of the chemical reactivity of the metalloporphyrin dimer cations is in progress. We view this work as an important step in the quest for a better understanding of the chemical and physical properties of metalloporphyrin dimers.

Experimental Section

Reagents and Solvents. All solvents were distilled from sodium benzophenone ketyl (THF, benzene, DME, and hexane) or from P_2O_5 (CH_2Cl_2) and stored under nitrogen. Dichloromethane- d_2 was dried through a neutral aluminum column and acetonitrile- d_3 over molecular sieves; benzene- d_6 was distilled from sodium benzophenone ketyl. NMR solvents were degassed by successive freeze–pump–thaw cycles on a high-vacuum line (10^{-5} torr). Tris(4-bromophenyl)ammonium hexachloroantimonate (TBPAAH) and silver tetrafluoroborate were purchased from Aldrich and used without further purification. Tetrabutylammonium perchlorate (TBAP) was prepared from tetrabutylammonium bromide and perchloric acid, recrystallized at least six times from 95% EtOH and dried overnight at 80 °C in vacuo. The syntheses of $[Ru(OEP)]_2^1$ and $[Os(OEP)]_2^2$ have been described previously. Ferrocenium hexafluorophosphate ($[FeCp_2](PF_6)$) was prepared by the procedure of Yang et al.³²

UV–vis spectra were recorded on a Cary Mode 219 recording spectrophotometer. The extinction coefficients were determined in dichloromethane (or acetonitrile) containing a sample at a concentration of 6.5×10^{-5} M. ¹H NMR spectra were obtained on a 300 MHz wide-bore Nicolet Supercon with a Model 1280 E FT disk data system. ESR spectra were recorded on a Bruker ER220D-SRC. Electrochemical experiments were performed with standard three electrode cells and instrumentation in approximately 10^{-3} M solution of the sample in either 0.8 M Bu_4NClO_4/DME or 0.2 M Bu_4NClO_4/CH_2Cl_2 . To avoid the rapid decomposition of the neutral dimers in CH_2Cl_2 the cyclic voltammograms were recorded as soon as possible after the preparation of the solution (~20 s). All manipulations and syntheses were performed in a Vacuum Atmospheres inert atmosphere box with an oxygen level of less than 2 ppm. Mass spectrometry (fast atom bombardment) was performed at the University of California-San Francisco Bio-Organic, Biomedical Mass Spectrometry Resource.

Bis(octaethylporphyrinato)ruthenium(II,III) Tetrafluoroborate (1). $AgBF_4$ (4 mg, 0.020 mmol) was dissolved in 1 mL of THF and added dropwise to a well-stirred solution of $[Ru(OEP)]_2$ (27 mg, 0.021 mmol) in 10 mL of benzene. The final solution was stirred for 3 h. The precipitate was filtered through a fine frit and washed with benzene and hexane. The purple solid was a mixture of the desired product and AgO powder. To remove the silver the precipitate was washed with CH_2Cl_2 , leaving a gray solid (metallic Ag) on the frit. The volume of the CH_2Cl_2

solution was reduced, and hexane was added until precipitation occurred. The resulting purple powder was filtered, washed with hexane, and dried under vacuum (20 mg, 73%): NMR (CD_2Cl_2) H_{meso} 12.91 (s), CH_2 9.92 (m), 5.65 (m), CH_3 2.15 (7.5 Hz, t) ppm; UV–vis (CH_2Cl_2) λ_{max} (log ϵ) 346 (5.26) (Soret), 384 (sh), 476 (4.14), 504 (sh), 546 (4.02), 572 (4.02), 644 (3.87) nm. Anal. Calcd for $C_{72}H_{88}BF_4N_8Ru_2$: C, 63.84; H, 6.55; N, 8.27. Found: C, 63.56; H, 6.49; N, 8.22.

Bis(octaethylporphyrinato)ruthenium(III,III) Tetrafluoroborate (7). $AgBF_4$ (8.4 mg, 0.043 mmol) was dissolved in 3 mL of THF and added to a solution of $[Ru(OEP)]_2$ (26 mg, 0.020 mmol) in 10 mL of benzene; precipitation occurred immediately. The purple solid was collected and purified as in the preparation of **1** (28 mg, 95%): NMR (CD_2Cl_2) H_{meso} 9.86 (s), CH_2 4.49 (m), 4.25 (m), CH_3 1.61 (7.5 Hz, t) ppm; UV–vis (CH_2Cl_2) λ_{max} (log ϵ) 347 (5.21) (Soret), 388 (sh), 486 (4.06), 513 (4.07), 560 (4.02) nm. Anal. Calcd for $C_{72}H_{88}B_2F_8N_8Ru_2$: C, 60.00; H, 6.15; N, 7.77. Found: C, 59.21; H, 5.89; N, 7.62.

Bis(octaethylporphyrinato)ruthenium(II,III) Hexafluorophosphate (2). A suspension of $[FeCp_2](PF_6)$ (4.5 mg, 0.014 mmol) in 1 mL of THF was added to a solution of $[Ru(OEP)]_2$ (19 mg, 0.015 mmol) in 10 mL of benzene. The reaction mixture was stirred overnight. The solid that formed was filtered, washed copiously with benzene, and recrystallized from CH_2Cl_2 –hexane. The resulting purple powder was collected by filtration, washed with hexane, and dried under vacuum (17 mg, 88%): NMR (CD_2Cl_2) H_{meso} 12.91 (s), CH_2 9.94 (br s), 5.64 (m), CH_3 2.15 (7.5 Hz, t) ppm; UV–vis (CH_2Cl_2) λ_{max} (log ϵ) 345 (5.10) (Soret), 384 (sh), 474 (4.01), 5.04 (sh), 546 (3.89), 568 (3.89), 642 (3.72) nm. Anal. Calcd for $C_{72}H_{88}F_6N_8PRu_2$: C, 61.22; H, 6.28; N, 7.93. Found: C, 62.16; H, 6.24; N, 7.44.

Bis(octaethylporphyrinato)ruthenium(III,III) Hexafluorophosphate (8). A suspension of $[FeCp_2](PF_6)$ (14 mg, 0.044 mmol) in 2 mL of THF was added to a solution of $[Ru(OEP)]_2$ (25 mg, 0.020 mmol) in 10 mL of benzene. The reaction mixture was stirred overnight. The purple solid that formed was collected and purified as for **2** (29 mg, 96%): NMR (CD_2Cl_2) H_{meso} 9.86 (s), CH_2 4.49 (m), 4.25 (m), CH_3 1.61 (7.5 Hz, t) ppm; UV–vis (CH_2Cl_2) λ_{max} (log ϵ) 347 (5.20) (Soret), 388 (sh), 486 (4.05), 514 (4.05), 560 (4.01) nm. Anal. Calcd for $C_{72}H_{88}F_{12}N_8P_2Ru_2$: C, 55.52; H, 5.69; N, 7.19. Found: C, 55.13; H, 5.49; N, 7.13.

Bis(octaethylporphyrinato)ruthenium(II,III) Hexachloroantimonate (3). A freshly prepared solution of TBPAAH (11 mg, 0.013 mmol) in 2 mL of THF was added to a solution of $[Ru(OEP)]_2$ (18 mg, 0.014 mmol) in 7 mL of benzene. The final solution was stirred overnight and filtered through a fine frit. The filtrate was evaporated to dryness, and the residue was recrystallized from THF–hexane. Filtration yielded purple-red crystals that were washed with hexane and dried under vacuum (17 mg, 78%): NMR (CD_2Cl_2) H_{meso} 12.93 (s), CH_2 9.96 (m), 5.66 (m), CH_3 2.16 (7.5 Hz, t) ppm; UV–vis (CH_2Cl_2) λ_{max} (log ϵ) 360 (sh), (5.12) (Soret), 504 (4.14), 530 (4.09) nm. Anal. Calcd for $C_{72}H_{88}Cl_6N_8SbRu_2$: C, 53.98; H, 5.53; N, 6.99. Found: C, 54.83; H, 5.73; N, 6.82.

Bis(octaethylporphyrinato)ruthenium(III,III) Hexachloroantimonate (9). A freshly prepared solution of TBPAAH (34 mg, 0.042 mmol) in 3 mL of THF was added to a solution of $[Ru(OEP)]_2$ (24 mg, 0.019 mmol) in 7 mL of benzene. The solution was stirred overnight. The precipitate was filtered, washed with THF, and recrystallized from acetonitrile–hexane. The purple-black powder was collected by filtration, washed with hexane, and dried under vacuum (22 mg, 60%): NMR (CD_3CN) H_{meso} 9.85 (s), CH_2 4.48 (m), 4.23 (m), CH_3 1.59 (7.5 Hz, t) ppm; UV–vis (CH_3CN) λ_{max} (log ϵ) 355 (sh), 377 (4.93) (Soret), 3.96 (sh), 496 (4.21), 534 (sh), 629 (3.64) nm. Anal. Calcd for $C_{72}H_{88}Cl_{12}N_8Sb_2Ru_2$: C, 44.65; H, 4.58; N, 5.78. Found: C, 45.67; H, 4.45; N, 5.99.

Bis(octaethylporphyrinato)osmium(II,III) Tetrafluoroborate (4). $AgBF_4$ (3.3 mg, 0.017 mmol) was dissolved in 1 mL of THF and added to a solution of $[Os(OEP)]_2$ (26 mg, 0.018 mmol) in 10 mL of benzene. The solution was stirred for 5 h, and the purple precipitate was collected and purified as for **1** (19 mg, 72%): NMR (CD_2Cl_2) H_{meso} 8.49 (br s), CH_2 6.45 (br s), 5.15 (br s), CH_3 1.73 (br s) ppm; UV–vis (CH_2Cl_2) λ_{max} (log ϵ) 329 (4.77), 358 (4.90) (Soret), 488 (3.97) nm. Anal. Calcd for $C_{72}H_{88}BF_4N_8Os_2$: C, 56.42; H, 5.78; N, 7.31. Found: C, 55.66; H, 5.65; N, 7.16.

Bis(octaethylporphyrinato)osmium(III,III) Tetrafluoroborate (10). $AgBF_4$ (8.4 mg, 0.043 mmol) was dissolved in 3 mL of THF and added to a solution of $[Os(OEP)]_2$ (27 mg, 0.019 mmol) in 10 mL of benzene. Precipitation occurred immediately, and the resulting brown solid was collected and purified as for **1** (29 mg, 96%): NMR (CD_2Cl_2) H_{meso} 10.04 (s), CH_2 4.53 (m), 4.32 (m), CH_3 1.66 (7.5 Hz, t) ppm; UV–vis (CH_2Cl_2) λ_{max} (log ϵ) 333 (4.93), 358 (4.91), 449 (sh), 481 (4.09) nm. Anal. Calcd for $C_{72}H_{88}B_2F_8N_8Os_2$: C, 53.40; H, 5.47; N, 6.92. Found: C, 52.04; H, 5.31; N, 6.82.

Bis(octaethylporphyrinato)osmium(II,III) Hexafluorophosphate (5). A suspension of $[FeCp_2](PF_6)$ (3 mg, 0.009 mmol) in 500 μ L of THF

(31) Collman, J. P.; Brothers, P. J.; McElwee-White, L. M.; Rose, E. J. *Am. Chem. Soc.* **1985**, *107*, 6110.

(32) Yang, E. S.; Chan, M. S.; Wahl, A. C. *J. Phys. Chem.* **1975**, *79*, 2049.

was added to a solution of $[\text{Os}(\text{OEP})_2]$ (14 mg, 0.009 mmol) in 7 mL of benzene. The reaction mixture was stirred overnight. The purple solid was collected and purified as for **2** (11 mg, 76%): NMR (CD_2Cl_2) H_{meso} 8.49 (br s), CH_2 6.45 (br s), 5.15 (br s), CH_3 1.73 (br s) ppm; UV-vis (CH_2Cl_2) λ_{max} (log ϵ) 328 (4.71), 358 (4.83) (Soret), 488 (3.93) nm. Anal. Calcd for $\text{C}_{72}\text{H}_{88}\text{F}_6\text{N}_8\text{P}_2\text{Os}_2$: C, 54.36; H, 5.57; N, 7.04. Found: C, 54.88; H, 5.47; N, 6.69.

Bis(octaethylporphyrinato)osmium(III,III) Hexafluorophosphate (11). A suspension of $[\text{FeCp}_2](\text{PF}_6)$ (6 mg, 0.018 mmol) in 600 μL of THF was added to a solution of $[\text{Os}(\text{OEP})_2]$ (12 mg, 0.008 mmol) in 7 mL of benzene. Precipitation occurred immediately. The resulting brown solid was collected and purified as for **2** (14 mg, 97%): NMR (CD_2Cl_2) H_{meso} 10.01 (s), CH_2 4.49 (m), 4.32 (m), CH_3 1.66 (7.5 Hz, t) ppm; UV-vis (CH_2Cl_2) λ_{max} (log ϵ) 331 (4.81), 364 (4.75), 448 (sh), 481 (3.97) nm. No satisfactory elemental analysis was obtained for $\text{C}_{72}\text{H}_{88}\text{F}_{12}\text{N}_8\text{P}_2\text{Os}_2$.

Bis(octaethylporphyrinato)osmium(II,III) Hexachloroantimonate (6). A freshly prepared solution of TBPAAH (6.4 mg, 0.007 mmol) in 900 μL of THF was added to a solution of $[\text{Os}(\text{OEP})_2]$ (12 mg, 0.008 mmol) in 10 mL of benzene. The solution was stirred overnight. The purple solid was collected and purified as for **2** (10 mg, 72%): NMR (CD_2Cl_2) H_{meso} 8.47 (br s), CH_2 6.36 (br s), 5.09 (br s), CH_3 1.73 (br s) ppm; UV-vis (CH_2Cl_2) λ_{max} (log ϵ) 358 (4.58) (Soret), 3.92 (4.45), 500 (3.83), 5.96 (3.67) nm. Anal. Calcd for $\text{C}_{72}\text{H}_{88}\text{Cl}_6\text{N}_8\text{SbOs}_2$: C, 48.57; H, 4.98; N, 6.29. Found: C, 47.81; H, 4.71; N, 6.14.

Bis(octaethylporphyrinato)osmium(III,III) Hexachloroantimonate (12). A freshly prepared solution of TBPAAH (25 mg, 0.031 mmol) in 1.5 mL of THF was added to a solution of $[\text{Os}(\text{OEP})_2]$ (21 mg, 0.014 mmol) in 10 mL of benzene. Precipitation occurred immediately, and

the resulting brown solid was collected and purified as for **2** (29 mg, 94%): NMR (CD_2Cl_2) H_{meso} 9.78 (s), CH_2 4.48 (m), 4.29 (m), CH_3 1.72 (7.5 Hz, t) ppm; UV-vis (CH_2Cl_2) λ_{max} (log ϵ) 334 (sh), 355 (5.05) (Soret), 482 (sh), 537 (sh) nm. Anal. Calcd for $\text{C}_{72}\text{H}_{88}\text{Cl}_{12}\text{N}_8\text{Sb}_2\text{Os}_2$: C, 40.89; H, 4.19; N, 5.30. Found: C, 40.93; H, 4.07; N, 5.33.

Acknowledgment. This work was supported by grants from the National Science Foundation (CHE83-18512) and the National Institutes of Health (GM17880-15). Fellowship support for J. Prodoliet from the Swiss government is gratefully acknowledged. Assistance with the ESR experiments from Dr. L. McElwee-White and helpful discussions with J. M. Garner are gratefully acknowledged. NMR spectra were recorded on an instrument supported by the National Science Foundation (CHE81-09064). Mass spectrometry was performed at the Bio-Organic, Biomedical Mass Spectrometry Resource (A. L. Burlingame, Director), supported by the NIH Division of Research Resources Grant RR01614.

Registry No. 1, 101494-43-3; 2, 101494-44-4; 3, 101494-45-5; 4, 101494-47-7; 5, 101494-48-8; 6, 101494-49-9; 7, 101695-28-7; 8, 101695-29-8; 9, 101695-30-1; 10, 101695-25-4; 11, 101695-26-5; 12, 101695-27-6; TBPAAH, 40927-19-3; $[\text{Ru}(\text{OEP})_2]$, 54762-43-5; $[\text{FeCp}_2](\text{PF}_6)$, 11077-24-0; $[\text{Os}(\text{OEP})_2]$, 89184-09-8; $[\text{Os}(\text{OEP})_2]^-$, 101652-23-7; $[\text{Ru}(\text{OEP})_2]^-$, 101652-27-1; $[\text{Os}(\text{OEP})_2]^{2-}$, 101652-22-6; $[\text{Ru}(\text{OEP})_2]^{2-}$, 101652-26-0; $[\text{Os}(\text{OEP})_2]^{3+}$, 101652-25-9; $[\text{Ru}(\text{OEP})_2]^{3+}$, 101652-29-3; $[\text{Os}(\text{OEP})_2]^{4+}$, 101652-24-8; $[\text{Ru}(\text{OEP})_2]^{4+}$, 101652-28-2; AgBF₄, 14104-20-2; Os, 7440-04-2; Ru, 7440-18-8.

Oxygenase Model Reactions. 1. Intra- and Extradial Oxygenations of 3,5-Di-*tert*-butylcatechol Catalyzed by (Bipyridine)(pyridine)iron(III) Complex

Takuzo Funabiki,* Akira Mizoguchi, Tsunemi Sugimoto, Shinichi Tada, Mitsuji Tsuji, Hiroyuki Sakamoto, and Satohiro Yoshida

Contribution from the Department of Hydrocarbon Chemistry and Division of Molecular Engineering, Faculty of Engineering, Kyoto University, Kyoto, Japan. Received August 27, 1985

Abstract: 3,5-Di-*tert*-butylcatechol (**1**) is oxygenated by (bipyridine)(pyridine)iron(III) complex with insertion of molecular oxygen to give intra- and extradiol oxygenation products. Isolation and reactivity of intermediate compounds have clarified that the intradiol oxygenation proceeds via a cyclic intermediate **4** to give a lactone **3** and the extradiol oxygenation via an acyclic intermediate **12** to form a lactone **5**. It has been shown that **12** gives thermally **10** and **6**. Products **7-9** are also formed. The stepwise insertion of oxygen rather than the one-step process via dioxetane intermediates has been clearly demonstrated by the ¹⁸O₂ tracer studies, especially by the insertion of one and two ¹⁸O atoms to **4** and **3**, respectively. Oxygenation mechanism involving the formation of a 1:1 catechol-iron complex, the oxygen attack on the catecholate ligand to form a catecholate ligand with a peroxide substituent, and oxygen insertion by the migration of the acyl group to the peroxide oxygen have been proposed. Formation of a 1:1 complex between **1** and iron(III) has been demonstrated by measurements of optical spectra. Reactivities of tris(3,5-di-*tert*-butylcatecholato)- and tris(3,5-di-*tert*-butylsemiquinonato)iron(III) complexes with oxygen and superoxide ion have supported the above mechanism.

Oxygenase, which plays important roles in the metabolic sequences of various organic substrates, has been studied extensively in recent years. Aside from works on monooxygenase and its model catalysts which function the epoxidation, hydroxylation, etc.,¹ there are many results on dioxygenase, which functions the cleavage of aromatic and indole rings, dihydroxylation, etc. Since the discovery of incorporation of an O₂ molecule into muconic acid in the oxygenation of catechol catalyzed by pyrocatechase,²

activation of molecular oxygen by coordination to iron in the iron-enzymes has widely attracted attention, but experimental evidences for the coordination of oxygen to iron have not been obtained.³ On the mechanism of oxygenation of catechols, the proposal of the one-step oxygenation via a dioxetane intermediate² seems to be superseded by that of the stepwise oxygenation via

(2) Hayaishi, O.; Katagiri, M.; Rothberg, S. *J. Am. Chem. Soc.* **1955**, *77*, 5450.

(3) (a) Que, L., Jr.; Lipscomb, J. D.; Zimmermann, R.; Munk, E.; Orme-Johnson, N. R.; Orme-Johnson, W. H. *Biochem. Biophys. Acta* **1976**, *452*, 320. (b) Que, L., Jr.; Lipscomb, J. D.; Munk, E.; Wood, J. M. *Ibid.* **1977**, *485*, 60. (c) Keyes, W. E.; Loehr, T. M.; Taylor, M. L.; Loehr, J. S. *Biophys. Res. Commun.* **1979**, *89*, 420.

(1) (a) *Molecular Mechanism of Oxygen Activation*; Hayaishi, O., Ed.; Academic Press: New York and London, 1974. (b) Guengerich, F. P.; MacDonald, T. L. *Acc. Chem. Res.* **1984**, *17*, 9. (c) White, R. E.; Coon, M. *J. Annu. Rev. Biochem.* **1980**, *49*, 315. Ullrich, V. *Adv. Inorg. Biochem.* **1979**, *119*. (c) Groves, J. T.; Nemo, T. E. *J. Am. Chem. Soc.* **1983**, *105*, 5786, etc.